Nanoclay Modification and Functionalization for Nanocomposites Development: Effect on the Structural, Morphological, Mechanical and Rheological Properties

Marya Raji, Mohamed El Mehdi Mekhzoum, Abou el Kacem Qaiss and Rachid Bouhfid

Abstract During the last decades, a widespread research has been devoted to organically modified clay minerals as reinforcements for polymer matrices. The most commonly used procedure to prepare organophilic clay is the cation exchange reaction with ammonium surfactant. Nevertheless, this kind of surface modification does not provide an efficient covalent bond between clay minerals and polymer matrices. For these reason, wide variety of silane coupling agents has been used to achieve compatibility and good dispersion between the hydrophilic clay and hydrophobic polymer. In this respect, the obtained polymer/organoclay nanocomposites exhibit significant improvements in their physical and mechanical properties over those of raw polymers. Herein, this chapter is divided into two parts. In the first part, it focus on the effect of silane modification of different clays minerals namely Halloysite, Montmorillonite and Sepiolite by various organosilanes such as 3-aminopropyltrimethoxysilane (A), 3-iodopropyltrimethoxysilane (I), 3-mercaptopropyltrimethoxysilane (S) and triethoxyvinylsilane (T). Although the silylation method, characterization and properties of the silane grafted clays are discussed. The second part is devoted to the preparation of polymer/silane grafted clay nanocomposites by melt compounding using polypropylene as polymer matrix. From the nanocomposites with 3wt% concentration in terms of silane grafted clay produced, the morphological, physical, mechanical, and rheological properties were measured. The results showed that the overall properties of silane grafted clays nanocomposites were increase which is attributed to better interfacial adhesion.

M. Raji · M.E.M. Mekhzoum · A.e.K. Qaiss · R. Bouhfid (✉)
Moroccan Foundation for Advanced Science, Innovation and Research (MAScIR),
Laboratory of Polymer Processing, Rabat Design Center, Institute of Nanomaterial
and Nanotechnology (NANOTECH), Rue Mohamed El Jazouli, Madinat Al Irfane,
10100 Rabat, Morocco
e-mail: r.bouhfid@mascir.com

1 Introduction

Because of the surge in the field of nanotechnology, polymer matrix based nanocomposites have recently become a promising current research field in the worldwide. These new kinds of materials have attracted steadily growing interest in numerous industrial applications, mainly in the transportation sector, building/construction industries and food packaging plastics (Galpaya 2012). They often exhibit remarkable properties, including unique mechanical and electrical conductivity, high gas and liquid barrier, flame retardant and thermal properties as compared to the neat polymers (Yeh and Hwang 2006).

The development and progression of environmentally friendly/green nanocomposites materials, will not only benefit on the plastic industry, but would lead to reduce the percentage of the expensive polymer used in the manufacture of materials, such as polypropylene, polyacrylic, polyester and epoxies etc. (Alonso et al. 2012). They are hazardous to the environment, non-degradable and take a long time to decompose, which generates huge many environmental problems associated with their disposal, including damage to the environment eco-system, water supplies, and sewer systems as well as to the lakes, rivers and streams. Furthermore, they are non-renewable; and their high price and unstable with impending depletion of petroleum resources (Majeed et al. 2013).

The incorporation of nano-sized particles in the polymer nanocomposites can reduce their production cost, through the substitution of small amount of polymer by a cheap and abundant resource may be organic or inorganic include layered materials such as graphite, and some clay types, or fiber-like materials namely carbon nano-tubes and nano-fibers, cellulose nano-fibers or other types of clay (Šupová et al. 2011). Among these particles loading, the different kinds of clay reinforcement have been proven an unavoidable synergistic impact on the overall performance of the nanocomposites, due to its special structure, which are most thermally stable and it arranged on the nanometer scale with a high aspect ratio and/or an enormously large surface interface with polymer. In this regard, the low cost, less weight, and low moisture absorption and also the low density makes the clay an attractive alternative to organic or petrochemical-based loading (El Achaby et al. 2013).

Since, discovered the possibility to build a polymer clay nanocomposite in the late 1980s (Nguyen and Baird 2007). Several investigations have also been conducted regarding on the development of new advanced and find further applications. The Toyota Research team began the investigations into reinforcing polymers; they found that the incorporation of moderate mineral clay charge into Nylon 6 marked the stimulus for subsequent theoretical and applied over the last decades, followed by Vaia observations (Vaia et al. 1993), that reported it is

possible to melt mixing polymers and clays without organic solvents. These two important results have motivated both academic and industrial labs to focus their attention on the polymer/clay nanocomposites.

2 Clay Minerals: Structure, Properties and Applications

To fully understand the effect of clay reinforcement on the polymer matrix properties, it is important to highlight the clay definition and their structure. The term clay mineral is difficult to define. From chemical point of view, this term signifies a class of the broad category of hydrated phyllosilicates, likewise, based on geological knowledge, this clay making up the fine-grained fraction of rocks, sediments, and soils (Velde 1985). Far from this definition which create some ambiguity until the moment, and for roughly speaking, clay minerals are essentially hydrous aluminosilicates with very fine particle size and a general chemical formula $(Ca, Na, H)(Al, Mg, Fe, Zn)_2(Si, Al)_4O_{10}(OH)_{2-x}H_2O$, where x represents the variable amount of water. Generally, the clay minerals may be broadly classified into two categories: natural and synthetic clays Include Montmorillonite, Hectorite, sepiolite, laponite, saponite, rectorite, bentonite, vermiculite, biedellite, kaolinite, chlorite, as a natural clays and the synthetic one such as various layered double hydroxides, synthetic Montmorillonite, Hectorite, etc. (Kotal and Bhowmick 2015). Figure 1 summarizes the major class of clay.

Generally, The different structures of clay minerals are basically composed of alternating of tetrahedral silica sheets "SiO_2" and alumina octahedral layers "AlO_6" in ratios of 1:1 when one octahedral sheet is linked to one tetrahedral sheet as Kaolinite, Halloysite, or in ratios of 2:1 this structure created from two tetrahedral sheets sandwiching an octahedral sheet such as Montmorillonite and Sepiolite, finally the proportion of 2:1:1 (chlorite), this latter are not always considered as
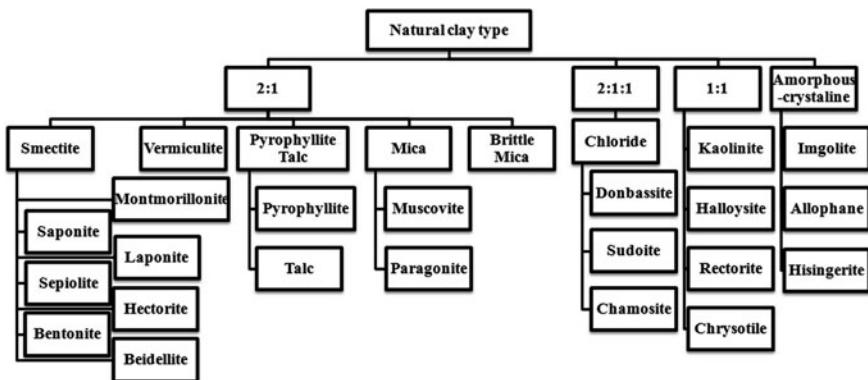

Fig. 1 Natural clay type

clay, sometimes being classified as a separate group within the phyllosilicates (García-López et al. 2010). One side of this lamella remains linked to each other through common oxygen atoms as seen in Fig. 2.

In consequently, the clay platelet undergoes a structural rearrangement to give different structures (nano-fibers, nano-tubes, and plate-like filler) as presented in Fig. 3.

The physical dimension of each platelet may be about 1 nm in thickness and the lateral dimension is varied from 30 nm to several micrometers or even larger, depending on particular silicate, due to an isomorphic substitution of alumina cation (Al^{3+}) within the silicate layers (Nguyen and Baird 2007). For example, in the case of 2:1 structure, the trivalent Al-cation in the octahedral layer is partially substituted by the divalent Mg-cation to form the Montmorillonite structure, given to each layer a net negative charge generated by their difference in valence (Paul and Robeson 2008). The negative charge is counter balanced by the interlayer alkali or alkaline earth metal cation as sodium and calcium ions, when these charges do not balanced and these ions do not fit in interlayer space, the mica will be formed and/or the layers organize themselves to form clay stalks and held together by relatively weak bonding forces of attraction between them as van der walls force, interstitial water and other polar molecules can placed inside the galleries, these latter can be then able to replace by organic cations, via a cationic-exchange reaction in the synthetic
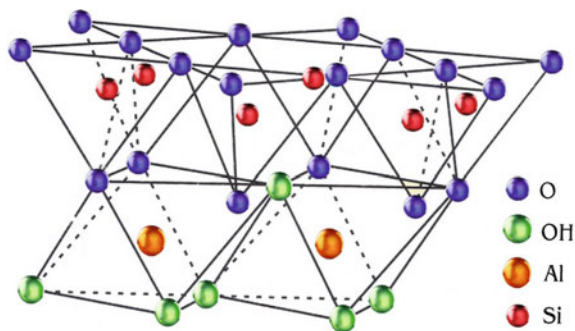
Fig. 2 Clay structure
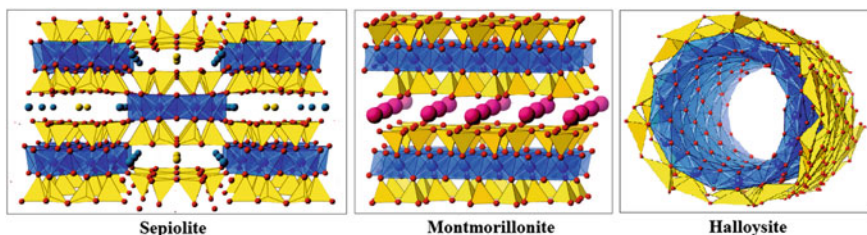
Fig. 3 Clay structures (nano-fibers, plate-like filler, and nano-tubes)

rout to transforms the hydrophilic-clay organophilic (Taxiarchou and Douni 2014). The gallery or the interlayer space of each kind of expansible clay is depend on the size and type of charge compensating cation and polar molecules on interior surfaces within the crystal clay structure itself, their presence on the basal planar rendering the clay hydrophilic in the nature (Bergaya and Lagaly 2013). Expansion of the space between two consecutive layers termed interlayers space, imparts high cation exchange capacity (CEC) relative to non-expansible phyllosilicates and most other secondary minerals (Yui et al. 2013).

Cation Exchange Capacity (CEC) is found to be an approximate measure of the amount of readily exchangeable cations neutralizing negative charge in the clay. Otherwise, it designed the capacity of the clay to hold cations, like Al^{3+}, Ca^{2+}, Mg^{2+}, Mn^{2+}, Zn^{2+}, Cu^{2+}, Fe^{2+}, Na^+, K^+ and H^+[14], it usually expressed formerly as milliequivalents per 100 g (meq/100 g), the CEC value differs from one clay to the other (Yui et al. 2013). A comparison of CEC values for some clay variety is provided in Table 1.

There are many methods available to determine the cation exchange capacity (CEC) of clay; any one is reliable employed for all clay powder. However, one possible technique that is used more effectively for all clay types is not dependent on the pH of saturation but is based on cation saturation, primarily the ammonium, sodium, and barium etc. as the index cation (Sanchez-Martin et al. 2006).

One main potential advantage of cation present between the clay layers is to be able therefore effectively replaced by organic cationic surfactant molecules, leads to renders clay useful in the large part of human existence (Hoidy et al. 2009). The initial application of clay minerals was more than 5000 years ago, for rheological additives, as thickeners in coating products, glues, platisols, drilling fluids and for wastewater treatment organoclays are used as thickeners in paints, greases, oil-base drilling muds, polymer composites and nanocomposites also for the purpose of gelling various organic liquids (Hoidy et al. 2009). Although there has been much work in the field of polymer/clay nanocomposites since their appearance (Liu and Wu 2001; Zeng et al. 2005; Mansoori and Hadi 2015), that will be detailed in the next paragraph.

Historical examples of clay nanocomposites applications are abundant in literature. Since antiquity, when Johnston had develop the fundamental concept of active sites and had also identified all the types of sites contributing to clay interaction with other substances, as in organoclays synthesis, include "broken edge" sites and exposed surface aluminol and silanol groups, isomorphic substitutions, exchangeable cations, hydrophobic silanol surfaces, hydration shell of exchangeable cations, and hydrophobic sites on adsorbed organic molecules (Rytwo 2008). The clay minerals become attractive to researchers, engineers and scientists as charge in many polymer industrial applications for commercial use. Thus, the era of clay/polymer nanotechnology can truly be said to have begun. The initial commercial application of clay nanocomposites was the use of clay, especially the Montmorillonite clay system to reinforce nylon-6 nanocomposites (He et al. 2010), used then as timing belt covers for Toyota cars, in collaboration with Ube in 1990 (Gao 2004). Unitika become the second producer of nylon-6 nanocomposites for

Table 1 Ranges of cation exchange capacities for clay

Clay types	Structure type	CEC (meq/100 g)	d-spacing (Å)	Chemical formula	R
Kaolinite	1:1(TO)	3–15	7.14	$[Si_4]Al_4O_{10}(OH)_8 \cdot nH_2O$ (n = 0 or 4)	(Alkan et al. 2005)
Halloysite	1:1(TO)	5–50	7	$[Si_4]Al_4O_{10}(OH)_8 \cdot nH_2O$ (n = 0 or 4)	(Sánchez-Fernández et al. 2014)
Illite	2:1(TOT)	10–40	10	$M_x[Si_{6.8}Al_{1.2}]Al3Fe_{0.25} Mg_{0.75}O_{20}(OH)_4$	(Euigyung et al. 2011)
Chlorite	2:1:1(TOT)	10–40	14	$(Al(OH)_{2.55})4[Si_{6.8}Al_{1.2}] Al_{3.4}Mg_{0.6}O_{20}(OH)_4$	(Bergaya and Lagaly 2013)
Montmorillonite	2:1(TOT)	60–150	12.4–17	$M_x(Al_{4-x}Mg_x)Si_8O_{20}(OH)_4$	(Navrátilová et al. 2007)
Vermiculite	2:1(TOT)	100–150	9.3–14	$M_x[Si_7Al]Al_3Fe_{0.5} Mg_{0.5}O_{20}(OH)_4$	(Kotal and Bhowmick 2015)
Hectorite	2:1(TOT)	120	12.4–17	$M_x(Mg_{6-x}Lix)Si_8O_{20}(OH)_4$	(Nguyen and Baird 2007)
Saponite	2:1(TOT)	86.6	12.4–17	$M_xMg_6(Si_{8-x}Alx)Si_8O_{20}(OH)_4$	(Hussain et al. 2006)
Sepiolite	2:1(TOT)	11–12	12	$Mg_4 Si_6 O_{15} (OH)_2 \cdot 6(H_2O)$	(Santos and Boaventura 2008)

engine covers on Mitsubishi's GDI engines in 1996 by using synthetic mica as the nano-fillers (Hussain et al. 2006). After that Chevrolet Impalas developed doors with thermoplastic polyolefin nanocomposite (TPO) (Hussain et al. 2006). This was followed by the announced of a step assistant component for GMC Safari and Chevrolet Astro vans16 as the first application of clay/polyolefin nanocomposites of General Motors and Basell (Tjong 2006). More recently, Noble Polymers has developed clay/polypropylene nanocomposites for structural seat backs in the Honda Acura17, while Ube is developing clay/nylon-12 nanocomposites for automotive fuel lines and fuel system components; the following table summarizes some commercial polymer nanocomposites (Gao 2004).

As summarized in the Table 2, the clay nanocomposites are really commonly used in the wide plastic industry due to its attractive versatility in terms of properties, precisely the synthetic one named organoclay, for instance, the great mechanical nanocomposites (tensile, stress, strain) properties together with a high thermal stability (Singla et al. 2012). The clay nano-fillers also can reduce the gas and liquid permeability (Soheilmoghaddam et al. 2014). Moreover, it can improve the dynamic mechanical performances, as well as the flame retardancy while retaining optical clarity of pure polymer (Ahmed Ben Hassan et al. 2014). Finally, the low cost and density, even at low filler loading (Pavlidou and Papaspyrides 2008).

As already mentioned in last paragraphs, there are six kinds of active sites which are important for explaining the mechanism during the synthesis of an organoclay (Pavlidou and Papaspyrides 2008). This reaction called functionalization is based on the interaction between clay minerals surface and organic components named surfactant through three different possible arrangements for their attachments to clay particles; firstly; the surfactant cations may are intercalated into the interlayer spaces by way of cation exchange and adhere to surface sites via electrostatic bonding-charge interaction, secondly; the surfactant cations and/or molecules are physically adsorbed onto the external surfaces of the particles to better coating the clay particles and finally; the surfactant molecules are located within the interlayer spaces (Pavlidou and Papaspyrides 2008). The studies on the organic surfactant grafted clay have been conducted after the introduction of X-ray diffraction in 1913 using different types of surfactant include (de Paiva et al. 2008): Anionic Surfactants, Nonionic, Cationic ones, and finally a single surfactant molecule display both anionic and cationic dissociations it is called amphoteric or zwitterionic.

These organic components can attach to the clay particles by different way is in depend on clay structure, the first one, is as organic surfactant which goes via ion exchange presented between clay layers (generally sodium and calcium ions) resulting in occupation of an interlayer space of the clay structure by organic molecules that hold positive chains and that will neutralize the negative charges from the clay layers (Beauvais et al. 2009). In order to introduce hydrophobicity and increase the clay basal space, which facilitate their exfoliation in the matrix and also improve the compatibility between the hydrophilic clay and hydrophobic polymer during extrusion. This clay modification called as organomodification, or also organophilization (Mejía et al. 2013). The second way of organic components attachment is as a compatibilizing agent if the clay structure does not contain an

Table 2 Commercial polymer nanocomposites. (Zeng et al. 2005)

Product	Characteristics	Applications	Producer
Nylon nanocomposites	Improved modulus, strength, heat distort temperature, barrier properties	Automotive parts (e.g., timing-belt cover, engine cover, barrier fuel line), packaging (e.g., cosmetics, food, medical, electronics), barrier film	Bayer, Honeywell Polymer, RTP Company, Toyota Motors, Ube, Unitika
Polyolefin nanocomposites	Stiffer, stronger, less brittle, lighter, more easily recycled, improved flame retardancy	Step-assist for GMC Safari and chevrolet Astro vans, heavy-duty electrical enclosure	Basell, Blackhawk Automotive Plastics, General Motors, Gitto Global Corporation, Southern Clay Products
M9™ Mitsubishi's MXD6 nylon	High barrier properties	Juice or beer bottles, multi-layer films, containers	Mitsubishi Gas Chemical Company
ORMLAS	High barrier performance, impact resistance, flame resistance, high clarity	Long-life food tray	Triton Systems
Durethan KU2-2601 (nylon 6)	Doubling of stiffness, high gloss and clarity, reduced oxygen transmission rate, improved barrier properties	Barrier films, paper coating	Bayer
Aegis™ NC (nylon 6/barrier nylon)	Doubling of stiffness, higher heat distort temperature, improved clarity	Medium barrier bottles and films	Honeywell Polymer
Aegis™ OX (nanoclay nylon 6 resins)	Highly reduced oxygen transmission rate, improved clarity	High barrier beer bottles	Honeywell Polymer
Aegis HFX	Highly reduced oxygen transmission rate	High barrier juice, tea, and condiments bottles	Honeywell Polymer
AEGIS CSD	High level of a passive carbon dioxide barrier	High barrier bottles weight	Honeywell Polymer
Specialty Film	Excellent barrier properties to oxygen, flavors, and aromas Provide toughness, strength, tear, and puncture resistance, and resistance to grease and gas penetration	Packaging applications: meat, fresh red meat, poultry, fish, cheese, dried food, and chilled fruit juices	Honeywell Specialty Polymers

Table 2 (continued)

Product	Characteristics	Applications	Producer
SET™ nanocomposite nylon 12	Improved stiffness, permeability, fire retardancy, transparency and recycling	Catheter shafts and balloons, tubing, film and barriers, flexible devices	Foster Corporation
Forte™ nanocomposite	Improved temperature resistance and stiffness, very good impact properties	Automotive, furniture, appliance	Noble Polymer

exchangeable cation, which is a graftization of the chemical element that has reactive groups compatible with another reactive groups existing on polymer chain to form the nanocomposite (Ferreira et al. 2011). The overall properties of the nanocomposites based on modified clay characteristics, commonly related on organic molecular mass, type and content of functional groups, organic components/clay proportion, and the manufacturing method (Lee et al. 2012). Among others, the chemical composition and the chain length of the functional groups that interact with the surface of the clays may improve many nanocomposites performance (Xie et al. 2010). The renowned using organic functional groups are Ammonium, phosphonium, imidazolium, Pyridinium, Sulfoniom, and the organosilanes (Leszczyńska et al. 2007). Amongst these latter the organosilanes are known as most favorable compatiblizers or coupling agents for clay fillers because they generally used for providing covalent bonding between clay fillers and polymer matrices, which enhance their interfacial adhesion, and then improve the mechanical properties of the nanocomposites (Sánchez-Fernández et al. 2014). A brief overview on organosilane chemistry and silylation of clay mineral is given below.

3   Oragnosilane Chemistry

Silicon is an essential element which has received a great attention due to is remarkably reactivity and its variety bonding possibilities (Bissé et al. 2005). Silicon is the second most ubiquitous element after oxygen, first, discovered in 1824 by Berzelius (Berzelius 1824). In fact, it is naturally found in the silica (SiO_2) or silicate forms (SiO_4) (Mai and Militz 2004). Silicon as a member of Group 14 in the periodic table shares numerous common characteristics with carbon, but also exhibits different chemical reactivity compared to carbon. Besides, much like carbon atoms, silicon can form four stable bonds with itself and other atoms. In contrast, silicon is more electropositive than carbon, which is much more susceptible of very special and unique chemical reactions. Owing to its dual reactivity, silicon molecule can be synthesized with the ability to bond both organic and

inorganic reactivity (Witucki 1993). Therefore, the unique chemical properties and performance characteristics of silicones give rise to variety of infinite silicon-based materials containing hybrid system of silicon/carbon known as 'Organosilane' (Verdejo et al. 2008).

Historically, it was not until 1907 that Kipping and coworkers reported the first synthesis of organosilane. They initially used organozinc, followed by Wurtz-type coupling (Na), before the use of the famous Grignard reagents to make the silicon-carbon bond as shown in Scheme 1. In 1943, Dow Corning Company began commercial development of organosilane technology, opening a new world in silicone chemistry and applications (Thomas 2011). In order to understand the interaction mechanisms between silane and clay minerals called "silylation", it is first necessary to look on the chemical structure of organosilane as coupling agent. See Scheme 1.

A silane is a monomeric silicon chemical similar to hydrocarbon. It has chemical formula $(R_1R_2R_3R_4)Si$ in which four chemical groups attached to the silicon atom. These groups can be the same or different, inorganic or organic and reactive or nonreactive (Halvorson et al. 2003). To be classified as an organosilane, at least one silane substituent must be an organic group linked to silicon through Si–C bond. Alternatively, organosilanes are currently available and unique class of organic silicon compounds; they can be classified according to their molecular and spacial structures. Organosilanes characterized by the $(R_1R_2R_3)SiX_n$ formula where n can have a value between 1 and 3, they possess a hydrolytically sensitive silicon based functional group SiX_n. Organosilanes compounds can form a variety of different hybrid organic-inorganic structures; they can react with other silanes, with themselves and with both inorganic and organic substrates via complex hydrolysis/condensation reactions. The R groups in organosilanes can be either nonreactive (hydrocarbon chain) or reactive substituent with terminal organofunctional groups (methacrylate, epoxy). These latter types of organosilanes compounds are bifunctional molecules and are referred to as silane coupling agents (Plueddemann 1991). In general, silane-coupling agents can be represented by the chemical formula, $Y–(R_1R_2R_3)–SiX_n$ in which at least one of the organic substituents R_1, R_2 and R_3 has a reactive organofunctional group Y. The most common silane coupling agent structures are functional organotrialkoxysilanes $(Y–R–SiX_3)$. Whereas sometimes, the trifunctional SiX_3 group can have only two or one X substituent namely

$$SiCl_4 + R_2Zn \longrightarrow SiR_4 \longleftarrow SiCl_4 + RMgBr$$

$$\Big\uparrow Na \qquad R = C_2H_5, C_6H_5$$

$$SiCl_4 + RBr$$
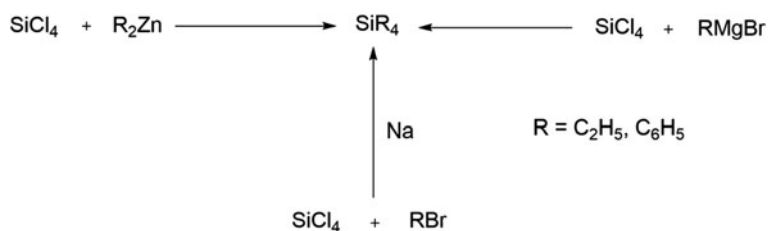
Scheme 1 Synthesis pathway for the preparation of organosilane compounds

Scheme 2 Different types of Functional organosilanes with varying numbers of hydrolyzable substituents on silicon

Trialkoxysilane   Dialkoxysilane   Monoalkoxysilane

Dipodal Silane
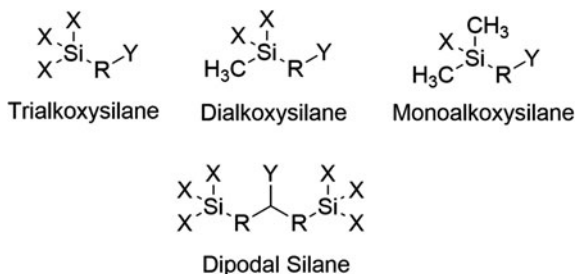
$Y–R_1R_2SiX_2$ and $YR_1R_2R_3SiX$ (Scheme 2). Silylating agents have usually three hydrolysable inorganic-reactive alkoxy groups, e.g., $–OCH_3$, $–OCH_2CH_3$, and one non-hydrolyzable organofucntional group such as amino, vinyl, mercapto. They have also an organo spacer group typically aryl or alkyl separates the organofunctional group from the silicon atom (Ishida and Kumar 1985). Typical commercial examples of silane coupling agents are illustrated in Table 3.

4 Silylation of Clay Minerals

As stated above, silane coupling agents are hybrid compounds with inorganic and organic constituents, they exhibit affinity for both organic and inorganic surfaces and act as a sort of intermediary to form a durable covalent bond between inorganic substrates (namely minerals, metals, cellulose and fillers) and organic polymer (such as thermoplastics or thermosets, rubber) (Weissenbach, Kerstin and Mack 2005). Figure 4 show the bifunctional silane coupling agent mechanism. Due to its unique dual reactivity, silylating agent can be useful for improving the adhesion between the two dissimilar materials (Matinlinna et al. 2013). Such silylating agent can find valuable application in the manufacture of pharmaceutical products, agro-chemicals and in electronics manufacturing (Blum 2003). In addition, any application where silane coupling agents are involved requires the silane molecule to be hydrolyzed and condensed.

Recently, silylation or silane grafting has proved to be an efficient way to modify clay minerals surfaces (Avila et al. 2010). Although, the interaction between hydrophobic molecules and clay could be greatly enhanced by simple grafting of hydrophibic silane groups onto the clay minerals (Takahashi and Kuroda 2011). As a result, the obtained silylation products exhibit suitable application in material science especially in polymer/clay nanocomposites (Isoda et al. 2000). In general, the interactions of silane coupling agents with clay minerals are mainly proceed through different steps. As shown in Scheme 3. Initially, the silane monomers react in the presence of water (hydrolysis) to form reactive, hydrophilic, acidic silanol groups Si–OH followed by partial condensation in which oligomers are formed; during the condensation, silane molecules react with each other forming dimers and

Table 3 Some Commercial silanes coupling agents with different organofunctional groups

Functional group	Chemical name	Structural formula
Epoxy	3-Glycidoxypropyltrimethoxysilane	
Amino	3-Aminopropyltriethoxysilane	
Mercapto	3-Mercaptopropyltrimethoxysilane	
Isocyanate	Tris-(trimethoxysilylpropyl) isocyanurate	
Chloroalkyl	3-Chloropropyltrimethoxysilane	
Diamino	Diaminopropyltrimethosysilane	
Methacryloxy	3-Methacryloxypropyltrimethoxysilane	
Vinyl	Vinyltrimethoxysilane	
Styryl	p-Styryltrimethoxysilane	
Acryloxy	3-Acryloxypropyl trimethoxysilane	

Fig. 4 Silane coupling agent mechanism
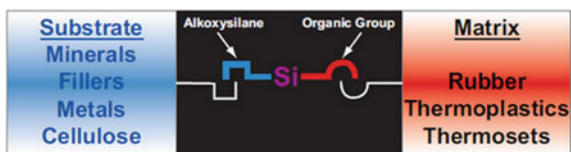
then condense to form siloxane oligomers. Next, the oligomers or monomers silanol are physically adsorbed to hydroxyl groups of clay minerals by hydrogen bonds on the clay surfaces. Finally, under dehydration condensation reaction a robust covalent bond –Si–O–Si– between silanols and hydroxyl groups of clays are formed during a drying process. Moreover, the covalent bond enables a durable
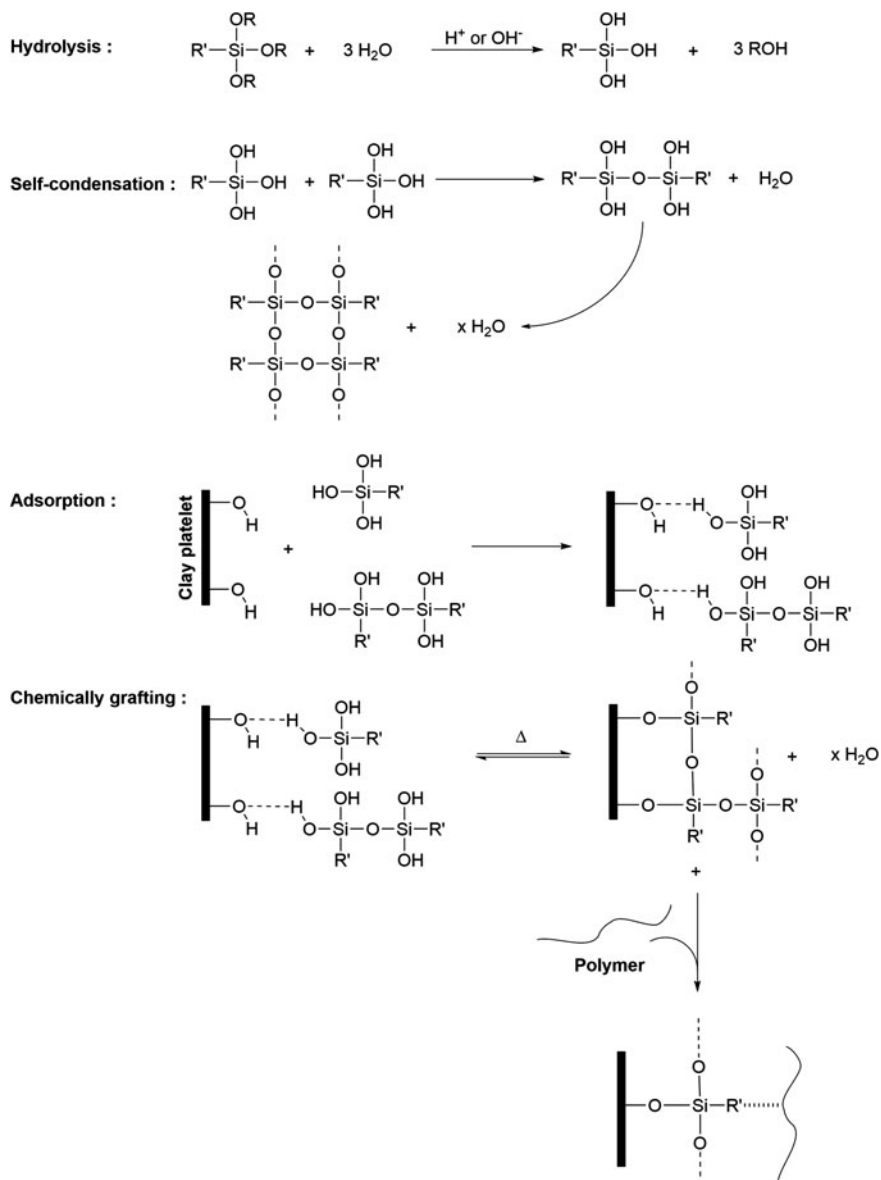
Scheme 3 A plausible mechanism of coupling reaction between silane grafted clay mineral and thermoplastic matrices

immobilization of the organic moieties in the silane grafted products which prevents their leaching into the surrounding solutions. In addition, the R' organofunctional group remains available can react with the polymer matrix, resulting in the

formation of a network among silane, clay mineral and polymer through covalent bonds. Therefore, the resultant polymer/clay nanocomposite exhibits a substantial improvement in their properties including mechanical, rheological and other handling properties (Shanmugharaj et al. 2006; Ha et al. 2007; Shen et al. 2007; Sánchez-Valdes et al. 2009). Certainly, the silanization of the clay mineral can take place at three basic models namely at the interlayer space, external surface and at the edges. The interlayer and edges grafting can increase the distance between the layers. For the external surface, the silylation has no effect on the basal spacing of the clay. Such successful silylation of clay minerals surfaces has been reported, in this case, a great attention was paid to the kind of silanes, the clay mineral structure as well as the influence of the solvents on the grafting reaction. In addition, the silanization reaction can also take place onto organoclay minerals to improve their compatibility with the polymer matrix (Park et al. 2004; Chen and Yoon 2005).

5 Preparation and Characterization of Silane Grafted Clay

In the present chapter, three different clay minerals were reported namely Montmorillonite lamellar structure, nano-fiber sepiolite and tubular Halloysite, a 1:1 layer silicate with rolled structural layers and interlayer water. Initially, the modifications of clays were carried out using four different commercial organosilanes. Although. Toluene was used as solvent for dispersing medium. Scheme 4 shows the chemical structure of the used silanes. Certainly, the choice of organosilane as coupling agent is determined by the nature and chemical structure of the thermoplastic matrices used. In our case, each silane differs by its organic functional groups such as vinyl (T), amino (A), iodo (I), and mercapto (S). These reactive groups can form chemical bonds with polymer materials. In addition, the interaction and the interfacial properties between polymer/clay depend on the type of the non-hydrolyzable organic moiety, which can affect the final macroscopic properties of the material obtained. The method of modifying clays presents; as an example; in this work has been performed in one step. The procedure consisted on dispersing an

Scheme 4 The schematic of the used silanes
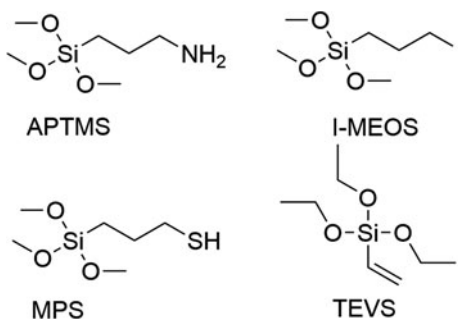
excess of clay (3 g) in 300 ml of toluene at 25 °C under constant stirring followed by sonication for at least 30 min. 3 ml of organosilane was introduced into the above-mentioned mixture and sheared for 24 h at 80 °C. After that, the modified clay was separated from solution by centrifugation at 10.000 rpm. The resultant product was washed using the mixture of ethanol/water for 3 times in order to remove the residual silane and dried at 60 °C in a vacuum oven. The final product was grinded and sieved before use.

5.1　X-Ray Diffraction (XRD)

Once the appropriate silane modified clays were prepared, a number of analysis techniques have been performed including XRD, FTIR, TGA analysis. First, XRD analysis was used to identify the chemical composition and crystallographic structure of the silane grafted clays. Figure 5 present the diffractograms of XRD of clay namely Halloysite, sepiolite and Montmorillonite as well as their four silane grafted -clays samples. As can be depicted from Fig. 5a, all diffractograms of the silane modified-Halloysite are almost identical and show no difference to the raw clays. The five solids are composed principally of two polymorphs of the bilaminar
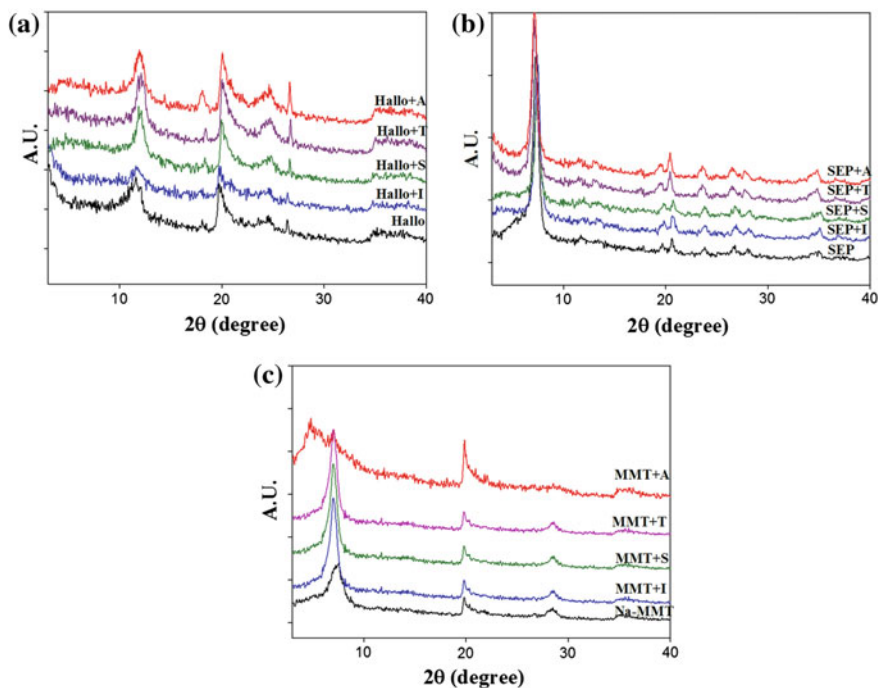

Fig. 5　XRD spectrum of montmorillonite, halloysite, sepiolite, and their silane grafted ones

clay (1:1) dioctahedral Halloysite, in the presence of SiO_2 and $Al(OH)_3$. In addition, both Halloysite-7A, and Halloysite-14A phases were identified. Therefore, during the process of silylation, the modification of Halloysite with different organosilanes did not cause any structural chemical changes compared to other clay minerals (Sánchez-Fernández et al. 2014). On the other hand, Fig. 5b show the XRD pattern of sepiolite which is affected by modification with organosilane. It can be seen that the intensities of some original peaks changed in the position range of 20–40 upon silylation. The variations in XRD diffractograms before and after the silylation of sepiolite show that there is a covalent bond formed by the interaction between sepiolite and different organosilanes, which can be confirmed by FTIR and TGA results (Belver et al. 2013). Figure 5c shows the XRD pattern of raw and silane grafted Montmorillonite. The MMT-A clay display a broad band around of $2\theta = 4.6°$. The interlayer spacing corresponding of the peak of MMT-Na around 1.21 nm which increased to 1.9 nm for the MMT-A clay, according to Bragg's equation (Eq. 1)

$$2d\sin\theta = n\lambda \qquad (1)$$

where,

λ is the wavelength of X-Ray, θ is diffraction angle and d is interlayer distance.

It can be concluded that, after clay modification by the organosilane (A), the ATPES molecule was intercalated and grafted to interlayer surface silanol groups. It can be mentioned that d-spacing value indicates a monolayers or paraffin-type arrangement between the aluminosilicate layers. This intercalation constitutes an efficient way to increase surface hydrophobicity which is a fundamental prerequisite for good compatibility between the polymer matrix and the Montmorillonite surface (Shen et al. 2007). For the others silane grafted Montmorillonite spectrum exhibits a broad band in the region between d = 1.31°, d = 1.32° and d = 1.26° for MMT-T, MMT-S and MMT-I, respectively. No significant differences were observed in the basal spacing of the latter modified clays. This observation may indicate that there are no interlayers or edges grafting, therefore, the silylation take place at the surface of the Montmorillonite which can be verified by FTIR and TGA results.

5.2 Structural Characteristics (FTIR)

The FTIR spectra of raw clays and the silane grafted ones by A, I, S and T silane molecules are presented in Fig. 6. Figure 6a shows the FTIR spectra of the Halloysite skeleton, The transmittance bands at 3697 and 3623 cm^{-1} in the FTIR spectrum were assigned to the stretching vibration due to O–H stretching of inner-surface hydroxyl groups, O–H stretching of inner hydroxyl groups of the Halloysite, respectively (Frost and Vassallo 1996). The interlayer water is indicated by the H–O–H (adsorbed water) deformation band appears at 1635 cm^{-1} (Bobos et al. 2001). The 1113 cm^{-1} peak was assigned to the stretching mode of Si–O, while
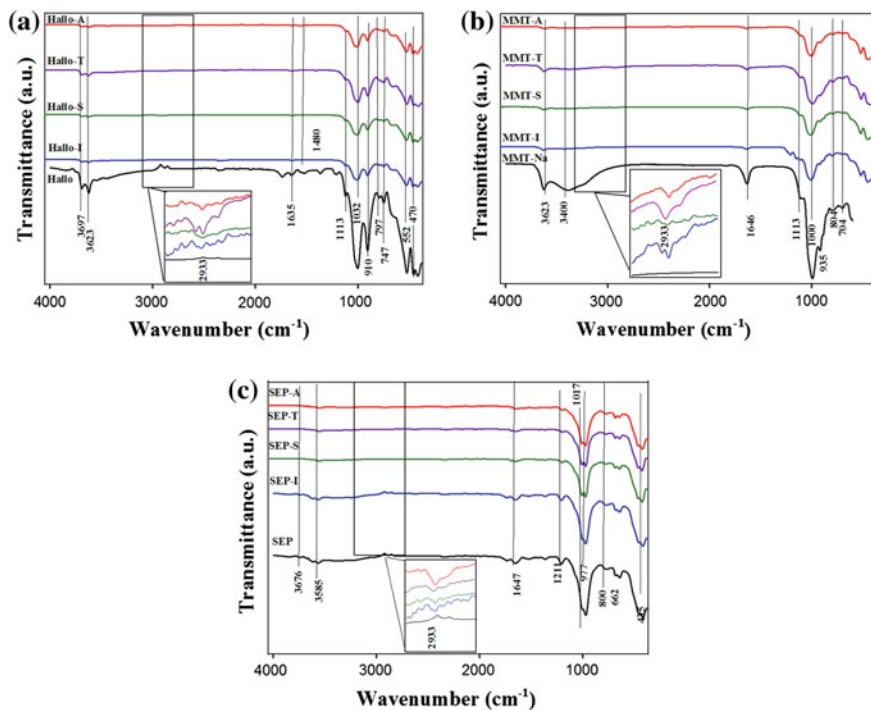
Fig. 6 FTIR spectra of montmorillonite, halloysite, sepiolite, and their silane grafted ones

the band at 1032 cm^{-1} was caused by the stretching vibration of Si–O–Si (Bordeepong et al. 2011). The O−H bending vibrations of the hydroxyl groups are observed at 910 cm^{-1} and Si–O–Si at 470 cm^{-1} confirm the existence of corresponding groups (Szczepanik et al. 2015). The bands attributed to the Al–OH vibrations of the surface hydroxyl groups are observed at 747 and 797 cm^{-1}. The band observed at 538 cm^{-1} was due to the vibration of Al–O–Si (Frost 1995). The Montmorillonite IR spectrum presented in Fig. 6b shows two important bands around 3623 and 3400 cm^{-1} which are indicative to O–H stretching for the silicate and water. The FTIR spectrum of clays, shows a band in the region of 1646 cm^{-1} which is attributed to the –OH bending mode of the adsorbed water (Xie et al. 2011). The characteristic band at 1113 cm^{-1} is assigned to Si–O stretching, and out-of-plane Si–O stretching mode of raw clays (Xie et al. 2011). The band at 1000 cm^{-1} is ascribed to Si–O stretching (in plane) vibration for layered silicates. The IR bands at 935, 804 and 704 cm^{-1} are attributed to Al–Al–OH, and Al–Mg–OH bending vibrations, respectively (Bhattacharya and Aadhar 2014). Figure 6c illustrates the FTIR spectrum of the sepiolite it shows the characteristic band at 3676 cm^{-1}, which is attributed to Mg–OH stretching of hydroxyl groups in octahedral Mg ions located in the interior blocks of natural sepiolite (Alan and İşçi 2014). The coordinated water corresponds of O–H stretching band appeared at 3585 cm^{-1}

and O–H stretching and deformation of zeolitic water bands observed for Sepiolite at 1647 cm^{-1} (Soheilmoghaddam et al. 2014). The Si–O coordination bands at 1211, 1017, 977 cm^{-1} are observed as a result of the Si–O vibrations (Ahmed Ben Hassan et al. 2014). The bands presented around 800 and 662 cm^{-1} are responsible from the O–H deformations and translations, respectively. The two peaks at 1017 and 435 cm^{-1} represent the stretching and bending of Si–O respectively in the Si–O–Si groups of the tetrahedral (Alan and İşçi 2014).

The FTIR spectrum of all silane grafted clays (sepiolite, halloysite and montmorillonite) detect other characteristic signals bands such as two weaker characteristics bands at 2933 cm^{-1} and at 2865 cm^{-1} attributed to aliphatic stretching of CH$_2$ and CH$_3$ groups, respectively. Another band at 1480 cm^{-1} which can be associated to the deformation vibration of CH$_2$ (Herrera et al. 2004), normally present in the mono- and the trifunctional silane molecules. Finally, the presence of silane in the all silane grafted clays spectrum is confirmed, which implies that silane has been grafted into the Montmorillonite, Halloysite and sepiolite structure.

5.3 Thermogravimetric Analysis (TGA)

The thermal degradation of the raw and silane grafted clays were evaluated by thermogravimetric analysis (TGA) to compare the degradation profiles of the different types of clay used as essential parameter in the choice of the technical applications of nanocomposite materials. The thermal decomposition of raw clays and the silane grafted ones by A, I, S and T silane molecules are superposed in Fig. 7. Firstly, the decomposition curves of the raw and silane grafted Halloysite can be divided in three steps as described in the following paragraph. Figure 7a shows the first weight loss for raw Halloysite in the range of 40–140 °C, which is reduced for the silane grafted ones, this lessen indicate an increase in the organophilicity of the Halloysite, while the adsorbed water content at the surface was reduced due to the presence of organosilanes. The second one in the range 200–320 °C can be attributed to the decomposition of silane bonded in the clay, and the decomposition of the oligomerized silane network that was not removed during washing. The last step is between 350–650 °C can be related to the structural dehydroxylation of the Al–OH and Si–OH groups and some additional organic decomposition of the silane grafted onto the Halloysite. Moreover, the higher weight loss shown from silane grafted Halloysites compared to raw Halloysite is consistent with the hydrocarbon chain of the alkyl group from the grafted silane molecules. This also supports the strong chemical interaction of the organosilanes with the Si–O and Al–O groups of Halloysite. The remaining materials at 800 °C (85 %) are of aluminum oxides and silicon oxides present in Halloysite structure. These results confirm the grafting of the silanes on the Halloysite (Carli et al. 2014).
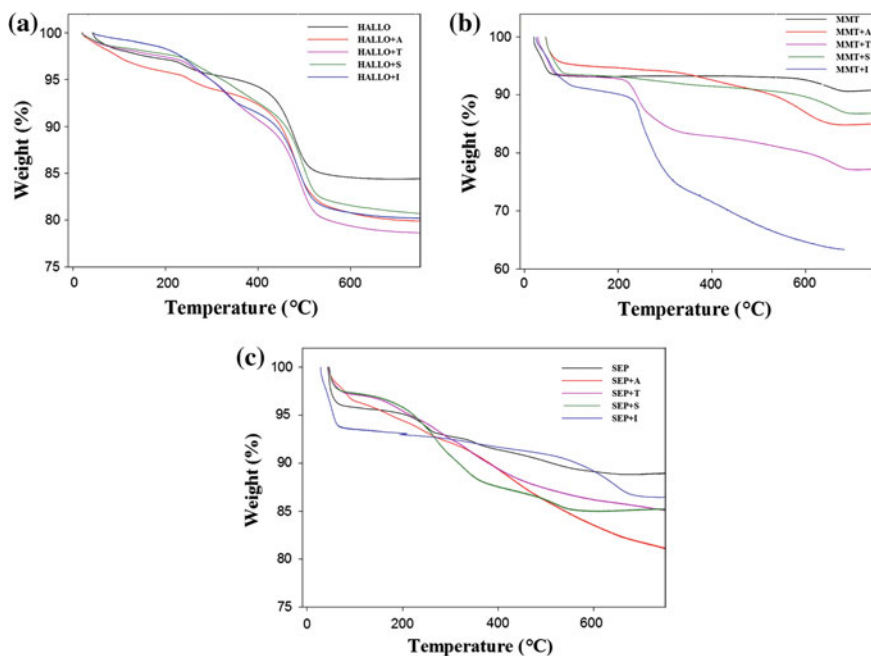
Fig. 7 TGA curves for the different raw and silane grafted clays used

The Montmorillonite thermal decomposition presented in Fig. 7, b) occurs in two steps: around 41 °C (7 % weight loss) and 651 °C (3 % weight loss) are due to the loss of physisorbed water and the loss of interstitially water, respectively. Another band appeared for silane grafted Montmorillonite ranging from 233 °C to 295 °C, in this region where the intercalated silane and all organic substances thermally decompose with a total weight loss varied from 2 % for MMT-A, 3 % for MMT-S, 10 % for MMT-T and 20 % for MMT-I.

The Grafted amount (mequiv/g), which corresponds to the amount of intercalated molecules which effectively participated in the silylation reaction, can be determined using Eq. 2 from the weight loss, W200–600, between 200 and 600 °C corresponding to silane degradation. The results show that the amount is varied from 1.17 for MMT-I, 0.37 for MMT-A, 0.53 for MMT-T and 0.74 for MMT-S (Zhao et al. 2009). (See Table 4)

$$\text{grafted amount (mequiv/g)} = 10^3 \, \frac{W_{200-600}}{(100 - W_{200-600})M} \qquad (2)$$

where M (g/mol) is the molecular weight of the grafted silane molecules.

Table 4 DTG bands of montmorillonite

Step	Bands	Characteristics	Sample name				
			Na-MMT	MMT-A	MMT-I	MMT-S	MMT-T
First step	loss of physisorbed water	T (°C)	41	56	78	75	56
		Mass loss (%)	7	5	9	7	7
Second step	decomposition of the intercalated silane	T (°C)	–	433	295	274	287
		Mass loss (%)	–	2	20	3	10
		Grafted amount (mequiv/g)	–	0.37	1.17	0.74	0.53
		Grafting yield (%)	–	25.1	27.35	35.9	30.1
Third step	loss of interstitially water	T (°C)	651	623	590	663	638
		Mass loss (%)	3	6	9	5	5

The grafting yield, which corresponds to the percentage of silane molecules which effectively participated in the silylated reaction, the following equation (Eq. 3) is employed, where [silane] (mequiv/ g) is the silane concentration in feed

$$\text{grafting yield } (\%) = \frac{\text{grafted amount } \times 100}{[\text{silane}]} \tag{3}$$

where [silane] (mequiv/g) designates the initial silane concentration.

Figure 8 shows the changes on sepiolite structure with thermal treatment, showing the importance of its water molecules. The thermal decomposition of neat sepiolite was carried out in four steps. First, below 250 °C, both zeolitic and adsorbed water could be eliminated in which the sepiolite structure remains

Fig. 8 DTG bands of sepiolite
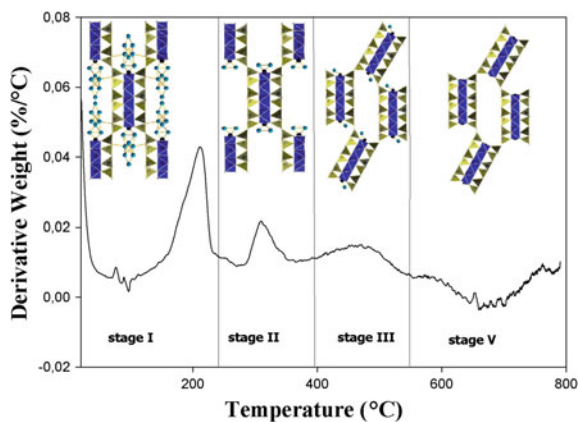
unchanged. Coordinated water is lost in two stages: between 250 and 350 °C and between 400 and 550 °C. Therefore, the coordination water loss involves structural changes reduction where a new channel cross-section of the zeolitic is reduced and an irreversible loss of water is produced. In this state, the mineral is called as anhydrous sepiolite. Between 550 and 1100 °C, the clay has lost all the water molecules and retains their Si–OH groups along its fiber. Above 1100 °C, the Si–OH was destroying after total dihydroxylation (Núñez et al. 2014). The TGA curves of both raw and silane grafted sepiolite are similar but an additional decomposition appears around 200–205 C. This new step close to the decomposition area of zeolitic water corresponds to the degradation of organosilane molecule, which is usually related to silane grafted on the silicate surface; these results confirm the silylation of sepiolite (Basurto et al. 2012), see Fig. 7c.

6 Nanocomposites Preparation

The characterization of each organoclays proved that all silane functionalization can modify the morphological and structural characteristics of the organoclay to better improve the mechanical and rheological properties of their nanocomposites, for revealing the successful surface modification and to evaluate the effect of silylation of organoclay nanocomposites, Herein we use the tensile and dynamic mechanical analysis (DMA) test results to reveal that both clay and the organoclay reinforced PP nanocomposites exhibited better properties than neat PP. The melt flow index (MFI) values will help to distinguish between the different grades of nanocomposite. Indeed, the scanning electron microscopy (SEM) images will be utilized to determine the particle size, morphological properties and their distribution/ dispersion into polymer matrix. Finally, the rheological test values will be also exploiting to characterize their visco-elastic behavior.

PP/unmodified and PP/ silane grafted clay nanocomposites were prepared by simple melt compounding using a Leistritz ZSE-18 twin-screw extruder (Leistritz Extrusiontechnik GmbH, Germany), under the following the temperature profile of the extruder barrel's seven zones was set from hopper to die at 170, 170, 175, 180, 180, 175, 170 and 170 °C, at 3wt% of each nano-clay were incorporate into PP via masterbatch process (10 % wt. nano-particles) obtained by the combination of PP with either MMT-Na, Halloysite, and Sepiolite and their organoclay by 3-aminopropyltrimethoxysilane (A) and triethoxyvinylsilane (T). After extrusion and pelletizing in a precision grinder (FRITSCH Pulverisette 19) into pieces of 2–3 mm, the compounds were injection molded using an Engel e-Victory injection molding machine with a 40 tons platen capacity. The process temperature of the injection press barrel was fixed at 180 °C while the nozzle temperature was set at 170 °C and mold at 45 °C. Then, the unmodified and the modified clay (A, T) nanocomposites were tested using different characterization methods as described next.

6.1 *Dynamic Light Scattering*

The clay nano-particles were evaluated by dynamic light scattering (DLS) to determine the particle size of different kind of clay which then may compared by modified clay particles size. The measurements were performed on a Zetasizer Nano ZS from Malvern Instruments Ltd. The Fig. 9 shows the dynamic light scattering of Halloysite, montmorillonite and sepiolite. The DLS result of Halloysite assumes that the particles have nanotube stricter with an average effective thickness around of 39 nm and a length about of 171 nm. In the other hand, the DLS result of the sepiolite and Montmorillonite clay, present that the both clay having the size about 264 nm and 171 nm, respectively.

6.2 *Scanning Electron Microscopy (SEM)*

In order to evaluate the effect of silylation treatments on clay morphology and the dispersion- distribution of the nanoclay in the matrix, scanning electronic microscopy (SEM) was used as a routine for morphology analysis of the nanocomposites polymer and provides much valuable information at the microscale level.
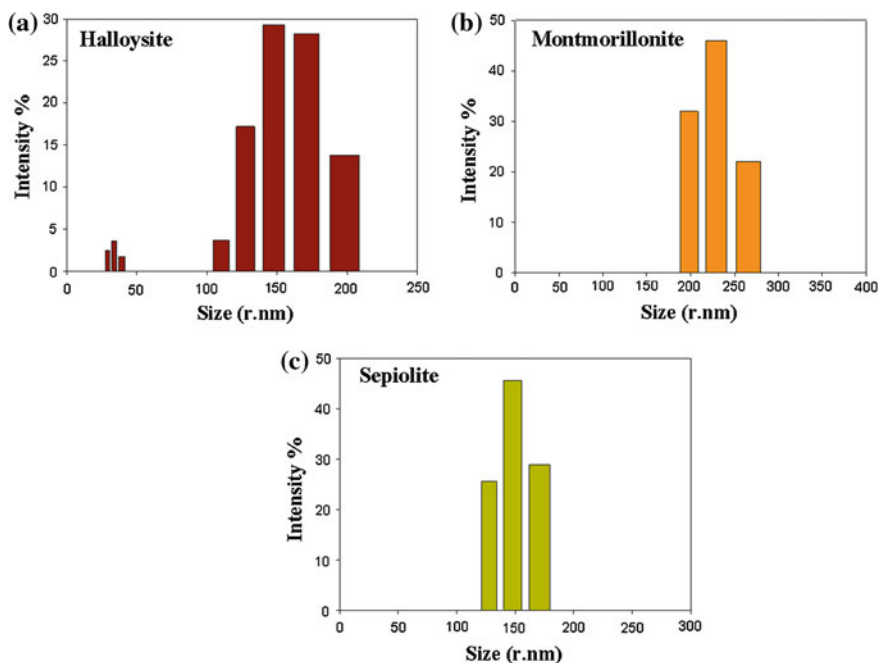

Fig. 9 Dynamic Light Scattering of **a** halloysite; **b** montmorillonite; **c** sepiolite

Some physical changes such as the size of nano-particles can be observed in Fig. 10, which illustrates the SEM images of the cry fracture surface of the nanocomposites reinforced by the raw and silane grafted clays. The all micrographs of silane grafted clays show that the clays nano-particles are uniformly dispersed in the PP matrix with a small amount of agglomerates, in contrast, it is observed on raw clays nanocomposites micrographs that there are a high number of agglomerations, resulting from the strong particle-particles interaction; the less aggregation and the lack of the voids around the clays nano-particles in the case of silane grafted clays nanocomposites indicate that the use of silane functionalization can improve the interfacial adhesion between the clays nano-particles and PP polymer matrix. Indeed, the use of melt compounding process to manufacture the nanocomposites is evident and enabled better nano-particles clay distribution. Based on these images, the size of 50 particles can be measured to get an average nanoparticles size summarized as follow in the Table 5. The particles sizes of all clays were decreased as compared to raw ones, attributed to the change of the clay structure by the silylation. The sizes of each clay particles measured by SEM are near of that measured by zetasizer, which means that they are no obvious agglomeration.

6.3 Melt Flow Index

The melt flow index (MFI) or melt flow rate (MFR) test was used to measures the uniformity of the flow rate of extrusion of a thermoplastic material through an orifice of specific length and diameter under prescribed conditions of temperature and load. The reported melt flow index values of each test specimen which was in the form of granules help to distinguish between the different grades of the nanocomposites. The MFI test was carried out following ASTMD1238-04, using the total load including the piston was 2.16 kg and melting temperature equal to 230 °C.

Figure 11, Shows that the MFI values of nanocomposites are increased compared to that of neat PP one, the addition of clay nano-particles illustrate an increase in flow of the polymers, this is due to the fact that the incorporation of clay nano-particles hinders plastic flow and decreases the viscosity of PP composites at the melt state. The MFI values of nanocomposites is then decreased by the chemical modification of clay, which may indicate that the structure of nano-particles was interconnected to hinder the molecular motion of polymer chains (Wang et al. 2013).
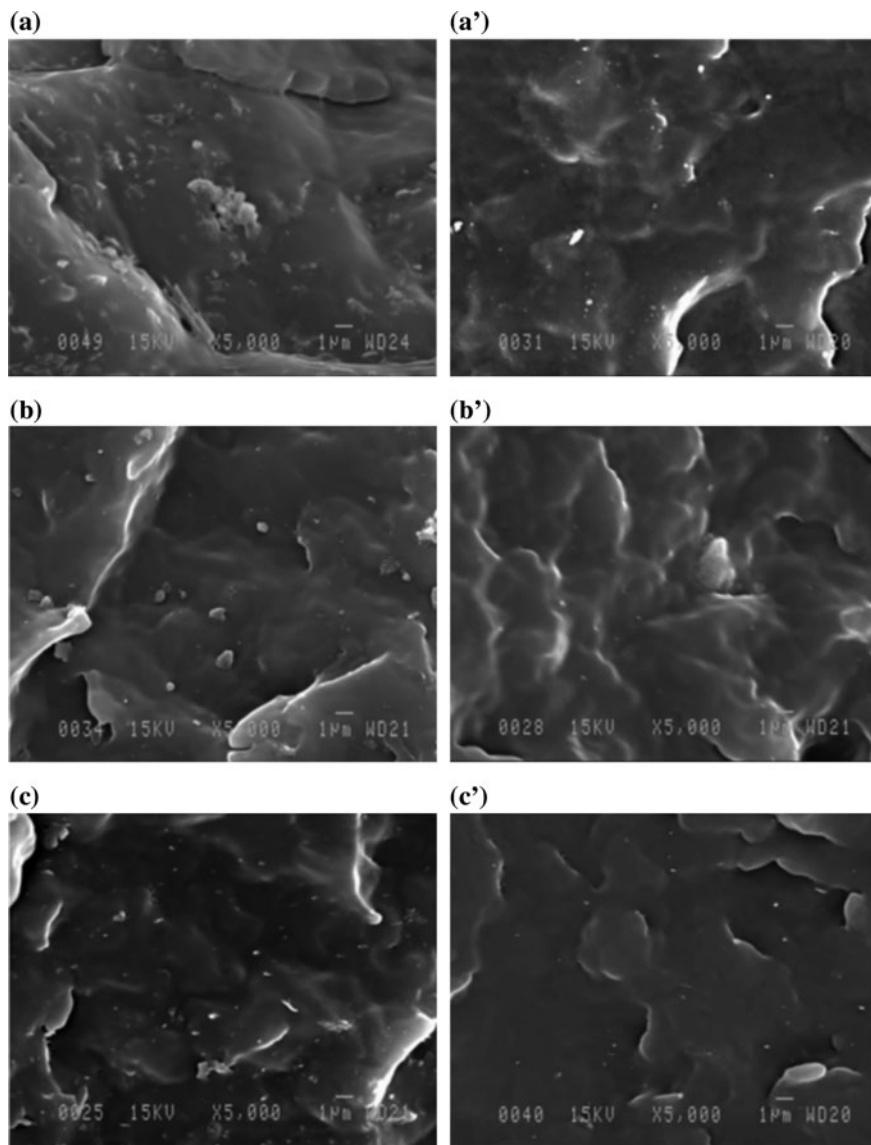
Fig. 10 SEM of **a** Halloysite; **b** grafted silane Halloysie; **c** Montmorillonite; **d** silane grafted Montmorillonite; **e** sepiolite; **f** silane grafted sepiolite

6.4 Tensile Testing

The mechanical test has been used to evaluate the improvement achieved by the silylation treatments of different clay on the nanocomposites properties. The device

Table 5 The average particles size of raw and modified clays nanocomposites from SEM analyses

| Clay nanocomposites		Particles size (nm)
Montmorillonite	Raw	305,73
	Modified	146,37
Halloysite	Raw	341,36
	Modified	257,16
Sepiolite	Raw	248,50
	Modified	134,21

Fig. 11 Effect of clay nano-particles and their chemical modification on the melt flow index of PP
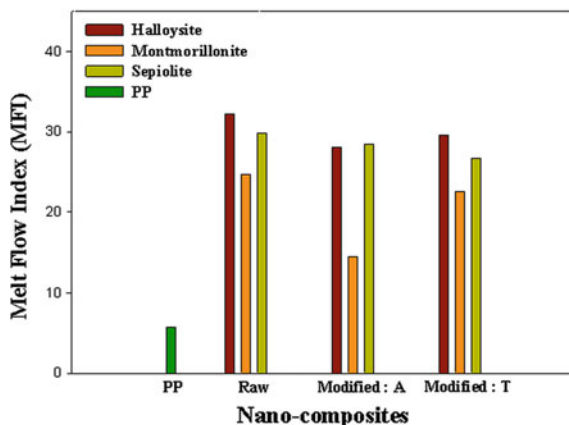
provides access to the force F exerted on the sample according to its elongation ΔL. The results can then be expressed in terms of the strain ε and stress σ. The tensile properties as Young's modulus, tensile strength and strain at yield of the nanocomposites were obtained from the stress-strain curves.

All specimens were tested using a universal test machine (H10KT, Tinius Olsen) with a cross head speed of 5 mm/min at room temperature. To investigate the effect of nanoclays loading and the effect of silane grafted clay on the mechanical properties of the manufactured nanocomposites, the tensile properties have been evaluated on terms of Young's modulus, tensile strength and strain at yield obtained from the stress-strain curves.

The Young's modulus of raw and silane grafted clays are showing in Fig. 12a. The Young's modulus values of each clay increase by the incorporation of clay and better by the silylated treatments of clay, the differences between silylated systems depending on the organosilane functional group responsible for interaction with the polymer matrix. The improvement of Young's modulus values in the case of unmodified clay from 1034 MPa of PP to 2176 MPa, 3220 MPa and 3117 MPa for Halloysite, Montmorillonite and sepiolite, respectively, is due to restricted mobility of polymer chains and their degree of freedom. These behaviors can be explained by the fact that there might be plenty of intermolecular covalent bonds formed between the surface of the clay and the polymer matrix, which enhance the
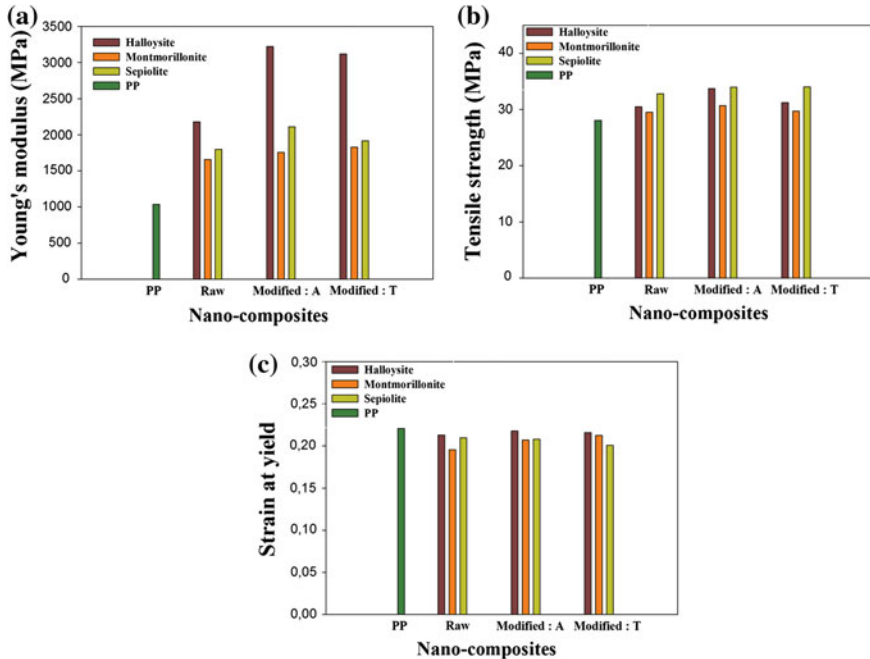
Fig. 12 Young's modulus, tensile strength and strain at yield of clay nano-particles and their chemical modification

adhesion between the composite components by the formation of a strong linkage between the organic and the inorganic phase (Kickelbick 2003).

The tensile strengths of raw and silane grafted clays with 3wt% clay content are shown in Fig. 12b. It's illustrated in Fig. 12b a marked increase in the tensile strength was observed for all nanocomposites Na-MMT, raw Halloysite and raw sepiolite at 3wt% up to 29.52 MPa, 30.05 MPa and 32.76 MPa, respectively, when compared to the neat polymer (28 MPa) which corresponds to a gain of 5 %, 7 % and 17 %, respectively. After silylation treatment, a clear increase of tensile strength values has been noticed compared to unmodified clay nanocomposites. This considerable enhancement in the tensile strength of the manufacturing nanocomposite cannot be explained only by uniformly dispersed clay particle with high aspect ratio and high intrinsic stiffness, but also can be ascribed to the strong interaction between nano-clay particles and polymer matrix (Zeng et al. 2005).

The dissimilar result has been observed from the clay nanocomposite for which the strain at Yield was be stable by the incorporation of nano-clay particles, the decrease of the strain at yield values from 22 % of the polymer composite to 21 %, 20 % and 21 % for Halloysite, Na-MMT and Sepiolite at 3 wt% clay content, respectively, correspond to a reduction of 3.48 % for Halloysite, 11.37 % Na-MMT and 5.09 % for Sepiolite, This can be allowed to concluded that the incorporation of clay at nanoscale does not affect the ductility of the produced nanocomposite. On

the other hand, Fig. 12c shows that, the strain at Yield was increase by the silylated treatments for all nanocomposites, It is believed that the improvement in stiffness and ductility of the nanocomposites is due to the homogenous dispersion of clay inside the polymer as well as the strong interaction between them, which facilitates enhancement of resistant to crack propagation so that higher strain can be tolerated by the nanocomposites (Carastan et al. 2013).

6.5 Torsional Test

Torsion tests were performed on an ARES-LS Rheometer using the rectangular torsion mode, with the following sample dimension: 5.5 mm width, 58 mm length, and 2 mm thick. Firstly, the strain sweep test was performed at 1 Hz frequency. Then, the torsion modulus is obtained in oscillatory tests performed at room temperature in sweep frequency mode (0.1–40 Hz) at strain of 2×10^{-3}, taken from the linear region of the strain sweep.

To investigate the nanocomposites response to shear stress; Fig. 13a–a" shows the torsion modulus for raw and silane grafted clays nanocomposites, for all systems, the torsion modulus increase with the incorporation of clay nano-particles. The addition of clay improved noticeably the G*values for all nanocomposite systems. Thus, the uses of silane organoclay nanocomposites increase the torsion modulus values as compared to raw clay nanocomposite, due to the improvement of the interfacial adhesion between the PP matrix and the nano-particles clays by the grafted silane. The variation of the torsional modulus is also marked by the variation of frequency from 0.1 to 40 Hz, leading to conclude that the nanocomposites response is like an elastic solid (Ganß et al. 2009).

To investigate the elastic and viscous behaviors of raw and silane grafted clay based nanocomposites, the evolution of tan δ versus frequencies and different kinds of clay nanocomposites (raw and modified clays) in Fig. 13b–b", for all nanocomposites tan δ decrease with increasing frequencies. Noteworthy is the curves in each system have the same shape with increasing frequency from 0.1 to 40 Hz. The elastic character of the nanocomposites prevails over a viscous behavior at high frequency. In the case of silane grafted clays, the tan δ values are lower than that of raw clay, which means that the silane grafted clays reduces the elastic character of nanocomposite and lead to a lower shear stress (Nekhlaoui et al. 2014).

6.6 Melt Rheological Test

The last paragraph is addressed to study the viscoelastic behavior of polymer nanocomposites in the solid state; nevertheless, it is necessary to analyze rheological behavior of specimen produced in the molten state to complete the observation made during compounding and to evaluate the microstructure and the
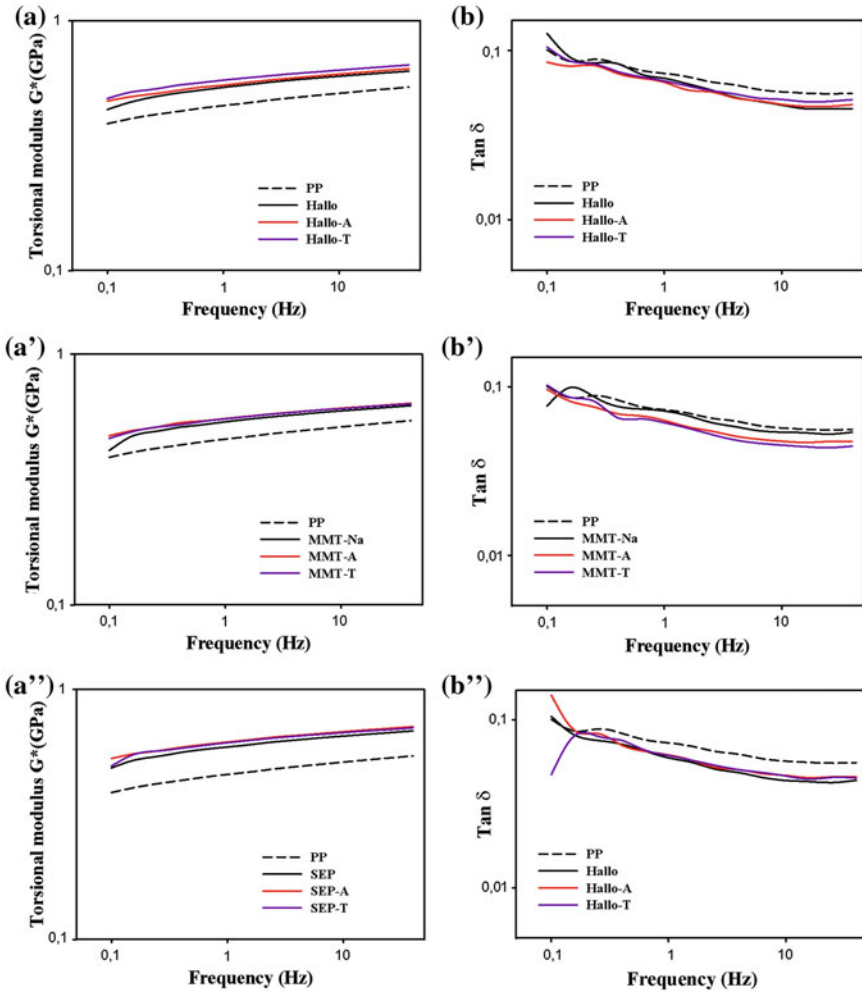
Fig. 13 The torsion modulus and tan δ of PP composites made with the raw and silane grafted clays at different frequencies

dispersion of nano-clay particles in the polymer matrix. The study of viscoelastic properties was made by means of the oscillatory melt rheology performed on an MCR 500 (Physica) rheometer equipped with a CTD600 device. The rheological measurements include the storage modulus G', loss modulus G" and tan δ were carried out at 190 °C under small amplitude oscillatory shear mode using 25 mm parallel plate-plate geometry with 1 mm thick samples. Frequency sweeps between 500 and 0.05 Hz were performed at a strain of 5 % (linear viscoelastic regime).

The rheological properties of the nanocomposites were also investigated in the melt state. Figure 14a–b" plots the storage modulus (G') and loss modulus (G") of
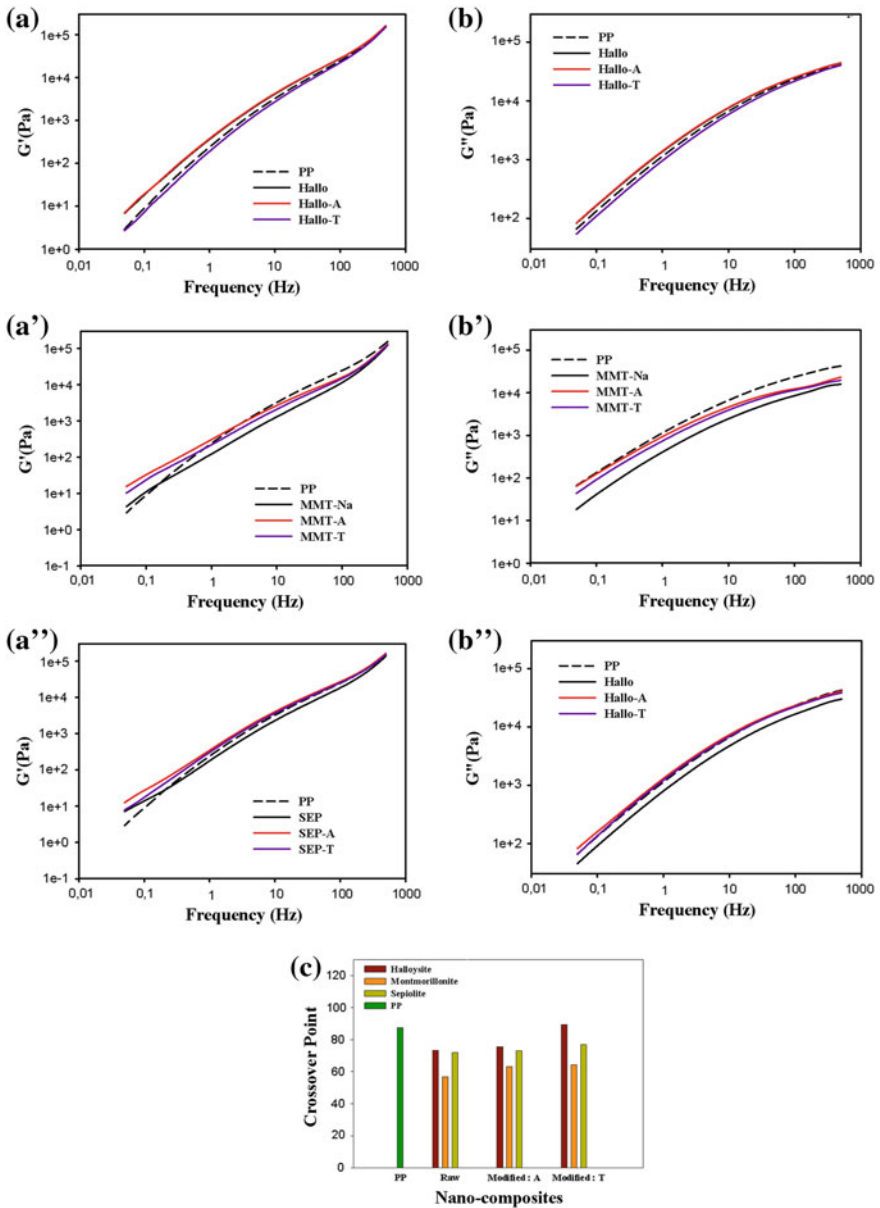
Fig. 14 Rheological properties as a function of PP composites made with the raw and silane grafted clays at different frequencies: **a**, **a'**, **a"** storage modulus, **b**, **b' b"** loss modulus, **c** crossover point

virgin PP nanocomposites made with the raw and silane grafted clays as function of frequencies. It is evident that both G' and G" increase linearly with an increase in angular frequency and it's clearly shows that G' values of the raw clays

nanocomposites are higher than that of pure and silane grafted clays nanocomposites. This can be explained by structural changes in the polymer nanocomposites, which being more elastic with rigid particle addition. However, in the presence of silane molecules grafted clays particles, the nanocomposites exhibit a high viscosity behavior due to the presence of organic chain grafted on nano-clays particles, and also due to the good dispersion, distribution and affinity of the rigid nano-clays inside the polymer blend, all these phenomena can prevent the melt to flow which is reflected by an increase in loss modulus/viscosity (Yürüdü et al. 2005). It also observed in Fig. 14a–b", for all nanocomposite at high frequency, that the G' values are higher than G" which indicates a solid-like response in the molten state. In fact, the insufficient time at higher frequency to allow polymer chains to relax contributing to an increase in the elastic nature of the melt (El Achaby et al. 2013).

Figure 14c shows the crossover frequency (G' = G") as a function of nanocomposites. The crossover point decreases by the incorporation of nano-clay particles indicating that the elastic behavior prevails over the viscous character due to the elastic character of nano-clays particles. However, in the case of silane grafted clays nanocomposites, the crossover point increase which meaning that the viscous behavior prevails over the elastic behavior as compared to raw clays nanocomposites, this reduction in nanocomposites rigidity can be explained by the grafted silane molecules on clays nano-particles and may be by the interaction between nano-clays particles and polymer matrix.

7   Conclusions

In summary, Polypropylene (PP)/organoclay nanocomposites have been prepared via melt compounding using a variety of clays such as raw and silane grafted Montmorillonite, Halloysite and sepiolite for purpose of comparison. First, various organosilanes were employed to produce organoclays structures with organophilic molecules in the presence of toluene solution. The dried organophilic clays were then melt-compounding with PP to obtain the corresponding PP/silane grafted clays nanocomposites. The successful silylation of different organosilanes onto the surfaces of clays were examined by various physico-chemical techniques, including FTIR, XRD, and TGA. Thus, suggesting the formation of chemical covalent bonding between the hydroxyl groups of clay minerals and alkoxy groups of silane grafted agent. In addition, the obtained SEM results showed clearly that the all clays were successfully modified using the silane molecules confirmed by lessen of the clay nano-particles size. Indeed, the MFI values was use to distinguish between the different grades of the nanocomposites. Finally, the silane grafted clays nanocomposites shows an improvement of the interfacial adhesion and random dispersion/distribution of clay nano-particles by the use of silane chemical modification afford remarkable composites property enhancements represented by high mechanical and torsional properties. It can be concluded that the functionalization

of nanoclay is mandatory to reach a high properties of nanocomposites and to benefit on the advantages of the nanoclays.

References

Ahmed Ben Hassan, S., Stojanović, D.B., Kojović, A., Janković-Castvan, I., Janaćković, D., Uskoković, P.S., Aleksić R.: Preparation and characterization of poly(vinyl butyral) electrospun nanocomposite fibers reinforced with ultrasonically functionalized sepiolite. Ceram. Int. **40**, 1139–1146 (2014)

Alan, N., İşçi, S.: Surface modification of sepiolite particles with polyurethane and polyvinyl alcohol. Prog. Org. Coat. **77**, 444–448 (2014)

Alkan, M., Hopa, Ç., Yilmaz, Z., Güler, H.: The effect of alkali concentration and solid/liquid ratio on the hydrothermal synthesis of zeolite NaA from natural kaolinite. Microporous Mesoporous Mater. **86**, 176–184 (2005)

Alonso, A., Bastos-Arrieta, J., Davies, G.: Ecologically friendly polymer-metal and polymer-metal oxide nanocomposites for complex water treatment. Nanocomposites—New Trends Dev. 187–213 (2012)

Avila, L.R., de Faria, E.H., Ciuffi, K.J., Nassar, E.J., Calefi, P.S., Vicente, M.A., Trujillano, R.: New synthesis strategies for effective functionalization of kaolinite and saponite with silylating agents. J. Colloid Interface Sci. **341**, 186–193 (2010)

Basurto, F.C., García-López, D., Villarreal-Bastardo, N., Merino, J.C., Pastor, J.M.: Nanocomposites of ABS and sepiolite: study of different clay modification processes. Compos. Part B Eng. **43**, 2222–2229 (2012)

Beauvais, M., Serreau, L., Heitz, C., Barthel, E.: How do silanes affect the lubricating properties of cationic double chain surfactant on silica surfaces? J. Colloid Interface Sci. **331**, 178–184 (2009)

Belver, C., Aranda, P., Ruiz-Hitzky, E.: Silica–alumina/sepiolite nanoarchitectures. J Mater. Chem. A **1**, 74–77 (2013)

Bergaya, F., Lagaly, G.: General Introduction: Clays, Clay Minerals, and Clay Science, 2nd edn. Elsevier Ltd (2013)

Berzelius, J.J.: Untersuchungen über die Flussspathsäure und deren merkwürdigsten Verbindungen. Ann. Phys. **77**, 169–230 (1824)

Bhattacharya, S.S., Aadhar, M.: Studies on preparation and analysis of organoclay nano particles. Res. J. Eng. Sci. **3**, 10–16 (2014)

Bissé, E., Epting, T., Beil, A., Lindinger, G., Lang, H., Wieland, H.: Reference values for serum silicon in adults. Anal. Biochem. **337**, 130–135 (2005)

Blum, F.D.: Silane Coupling Agents, Encyclopedia of Polymer Science and Technology, pp 38–50. Wiley, Inc. (2003)

Bobos, I., Duplay, J., Rocha, J., Gomes, C.: Kaolinite to halloysite-7 Å transformation in the kaolin deposit of São Vicente De Pereira, Portugal. Clays Clay Miner. **49**, 596–607 (2001)

Bordeepong, S., Bhongsuwan, D., Pungrassami, T., Bhongsuwan, T.: Characterization of halloysite from thung yai district, Nakhon Si Thammarat Province, in Southern Thailand. Songklanakarin J. Sci. Technol. **33**, 599–607 (2011)

Carastan, D.J., Amurin, L.G., Craievich, A.F., Gonçalves, C., Demarquette, N.R.: Morphological evolution of oriented clay-containing block co-polymer nanocomposites under elongational flow. Eur. Polym. J. **49**, 1391–1405 (2013)

Carli, L.N., Daitx, T.S., Soares, G.V., Crespo, J.S., Mauler, R.S.: The effects of silane coupling agents on the properties of PHBV/halloysite nanocomposites. Appl. Clay Sci. **87**, 311–319 (2014)

Chen, G.X., Yoon, J.S.: Clay functionalization and organization for delamination of the silicate tactoids in poly(L-lactide) matrix. Macromol. Rapid Commun. **26**, 899–904 (2005)

De Paiva, L.B., Morales, A.R., Valenzuela Díaz, F.R.: Organoclays: properties, preparation and applications. Appl. Clay Sci. **42**, 8–24 (2008)

El Achaby, M., Ennajih, H., Arrakhiz, F.Z., El Kadib, A., Bouhfid, R., Essassi, E., Qaiss, A.: Modification of montmorillonite by novel geminal benzimidazolium surfactant and its use for the preparation of polymer organoclay nanocomposites. Compos. Part B Eng. **51**, 310–317 (2013)

Euigyung, J., Won, L.J., Kyeong-won, S., Lee, Y.-S.: Effects of physicochemical treatments of illite on the thermo-mechanical properties and thermal stability of illite/epoxy composites. J. Ind. Eng. Chem. **17**, 77–82 (2011)

Ferreira, J.A.M., Reis, P.N.B., Costa, J.D.M., Richardson, B.C.H., Richardson, M.O.W.: A study of the mechanical properties on polypropylene enhanced by surface treated nanoclays. Compos. Part B Eng. **42**, 1366–1372 (2011)

Frost, R.L.: Fourier transform Raman spectroscopy of kaolinite, dickite and halloysite. Clays Clay Miner. **43**, 191–195 (1995)

Frost, R.A.Y.L., Vassallo, A.M.: The dehydroxylation of the kaolinite clay minerals using infrared emission spectroscopy. Clays Clay Miner. **44**, 635–651 (1996)

Galpaya, D.: Recent advances in fabrication and characterization of graphene-polymer nanocomposites. Graphene **01**, 30–49 (2012)

Ganß, M., Satapathy, B.K., Thunga, M., Staudinger, U., Weidisch, R., Jehnichen, D., Hempel, J., Rettenmayr, M., Garcia-marcos, A., Goertz, H.H.: Morphology and mechanical response of S—B star block copolymer—Layered silicate nanocomposites. Eur. Polym. J. **45**, 2549–2563 (2009)

Gao, F.: Clay/polymer composites: the story. Mater. Today **7**, 50–55 (2004)

García-López, D., Fernández, J.F., Merino, J.C., Santarén, J., Pastor, J.M.: Effect of organic modification of sepiolite for PA 6 polymer/organoclay nanocomposites. Compos. Sci. Technol. **70**, 1429–1436 (2010)

Ha, S.R., Ryu, S.H., Park, S.J., Rhee, K.Y.: Effect of clay surface modification and concentration on the tensile performance of clay/epoxy nanocomposites. Mater. Sci. Eng. A **448**, 264–268 (2007)

Halvorson, R.H., Erickson, R.L., Davidson, C.L.: The effect of filler and silane content on conversion of resin-based composite. Dent. Mater. **19**, 327–333 (2003)

He, A., Wang, L., Yao, W., Huang, B., Wang, D., Han, C.C.: Structural design of imidazolium and its application in PP/montmorillonite nanocomposites. Polym. Degrad. Stab. **95**, 651–655 (2010)

Herrera, N.N., Letoffe, J.M., Putaux, J.L., David, L., Bourgeat-Lami, E.: Aqueous dispersions of silane-functionalized laponite clay platelets. A first step toward the elaboration of water-based polymer/clay nanocomposites. Langmuir **20**, 1564–1571 (2004)

Hoidy, W.H., Ahmad, M.B., Al Mulla, E.A.J., Ibrahim, N.A.B.: Synthesis and characterization of organoclay from sodium montmorillonite and fatty hydroxamic acids. Am. J. Appl. Sci. **6**, 1567–1572 (2009)

Hussain, F., Hojjati, M., Okamoto, M., Gorga, R.E.: Review article: polymer-matrix nanocomposites, processing, manufacturing, and application: an overview. J. Compos. Mater. **40**, 1511–1575 (2006)

Ishida, H., Kumar, G. (eds.): Molecular Characterization of Composite Interfaces, 1st edn. Springer, US (1985)

Isoda, K., Kuroda, K., Ogawa, M.: Interlamellar grafting of γ-methacryloxypropylsilyl groups on magadiite and copolymerization with methyl methacrylate. Chem. Mater. **12**, 1702–1707 (2000)

Kickelbick, G.: Concepts for the incorporation of inorganic building blocks into organic polymers on a nanoscale. Prog. Polym. Sci. **28**, 83–114 (2003)

Kotal, M., Bhowmick, A.K.: Polymer nanocomposites from modified clays: recent advances and challenges. Prog. Polym. Sci. **51**, 127–187 (2015)

Lee, J., Man, S., Kim, J., Min, C.: Sensors and actuators B: chemical novel sulfonated styrenic pentablock copolymer/silicate nanocomposite membranes with controlled ion channels and their IPMC transducers. Sens. Actuators B Chem. **162**, 369–376 (2012)

Leszczyńska, A., Njuguna, J., Pielichowski, K., Banerjee, J.R.: Polymer/montmorillonite nanocomposites with improved thermal properties. Part II. Thermal stability of montmorillonite nanocomposites based on different polymeric matrixes. Thermochim. Acta **454**, 1–22 (2007)

Liu, X., Wu, Q.: PP/clay nanocomposites prepared by grafting-melt intercalation. Polymer **42**, 10013–10019 (2001)

Mai, C., Militz, H.: Modification of wood with silicon compounds. Inorganic silicon compounds and sol-gel systems: A review. Wood Sci. Technol. **37**, 339–348 (2004)

Majeed, K., Jawaid, M., Hassan, A., Abu Bakar, A., Abdul Khalil, H.P.S., Salema, A.A., Inuwa, I.: Potential materials for food packaging from nanoclay/natural fibres filled hybrid composites. Mater. Des. **46**, 391–410 (2013)

Mansoori, Y., Hadi, S.: Nanocomposite hydrogels composed of cloisite 30B-graft-poly(acrylic acid)/poly(acrylic acid): Synthesis and characterization. Poly. Sci. Ser. B **57**, 167–179 (2015)

Matinlinna, J.P., Choi, A.H., Tsoi, J.K.H.: Bonding promotion of resin composite to silica-coated zirconia implant surface using a novel silane system. Clin. Oral Implants Res. **24**, 290–296 (2013)

Mejía, A., García, N., Guzmán, J., Tiemblo, P.: Confinement and nucleation effects in poly (ethylene oxide) melt-compounded with neat and coated sepiolite nanofibers: modulation of the structure and semicrystalline morphology. Eur. Polym. J. **49**, 118–129 (2013)

Navrátilová, Z., Wojtowicz, P., Vaculíková, L., Šugárková, V.: Sorption of alkylammonium cations on montmorillonite. Acta Geodyn. Geomater. **4**, 59–65 (2007)

Nekhlaoui, S., Essabir, H., Kunal, D., Sonakshi, M., Bensalah, M.O., Bouhfid, R., Qaiss, A.: Comparative study for the talc and two kinds of Moroccan clay as reinforcements in polypropylene-SEBS-g-MA matrix. Polym. Compos. **36**, 675–684 (2014)

Nguyen, Q.T., Baird, D.G.: Preparation of Polymer—Clay Nanocomposites and Their Properties **25**, 270–285 (2007)

Núñez, K., Gallego, R., Pastor, J.M., Merino, J.C.: The structure of sepiolite as support of metallocene co-catalyst during in situ polymerization of polyolefin (nano)composites. Appl. Clay Sci. **101**, 73–81 (2014)

Park, M., Shim, I.K., Jung, E.Y., Choy, J.H.: Modification of external surface of laponite by silane grafting. J. Phys. Chem. Solids **65**, 499–501 (2004)

Paul, D.R., Robeson, L.M.: Polymer nanotechnology: nanocomposites. Polym. (Guildf) **49**, 3187–3204 (2008)

Pavlidou, S., Papaspyrides, C.D.: A review on polymer–layered silicate nanocomposites. Prog. Polym. Sci. **33**, 1119–1198 (2008)

Plueddemann, E.P.: Fundamentals of Adhesion. In: Lee, L.-H. (ed.) Fundamentals of Adhesion, pp. 279–290. Springer, US, Boston, MA (1991)

Rytwo, G.: Clay minerals as an ancient nanotechnology: historical uses of clay organic interactions, and future possible perspectives. Macla **9**, 15–17 (2008)

Sánchez-Fernández, A., Peña-Parás, L., Vidaltamayo, R., Cué-Sampedro, R., Mendoza-Martínez, A., Zomosa-Signoret, V., Rivas-Estilla, A., Riojas, P.: Synthesization, characterization, and in vitro evaluation of cytotoxicity of biomaterials based on halloysite nanotubes. Materials **7**, 7770–7780 (2014)

Sanchez-Martin, M.J., Rodriguez-Cruz, M.S., Andrades, M.S., Sanchez-Camazano, M.: Efficiency of different clay minerals modified with a cationic surfactant in the adsorption of pesticides: influence of clay type and pesticide hydrophobicity. Appl. Clay Sci. **31**, 216–228 (2006)

Sánchez-Valdes, S., Méndez-Nonell, J., Medellín-Rodríguez, F.J., Ramírez-Vargas, E., Martínez-Colunga, J.G., Soto-Valdez, H., Muñoz-Jiménez, L., Neira-Velázquez, G.: Effect of PEgMA/amine silane compatibilizer on clay dispersion of polyethylene-clay nanocomposites. Polym. Bull. **63**, 921–933 (2009)

Santos, S.C.R., Boaventura, R.A.R.: Adsorption modelling of textile dyes by sepiolite. Appl. Clay Sci. **42**, 137–145 (2008)

Shanmugharaj, A.M., Rhee, K.Y., Ryu, S.H.: Influence of dispersing medium on grafting of aminopropyltriethoxysilane in swelling clay materials. J Colloid Interface Sci. **298**, 854–859 (2006)

Shen, W., He, H.P., Zhu, J., Yuan, P., Frost, R.L.: Grafting of montmorillonite with different functional silanes via two different reaction systems. J. Colloid Interface Sci. **313**, 268–273 (2007)

Singla, P., Mehta, R., Upadhyay, S.N.: Clay modification by the use of organic cations. Green Sustain. Chem. **2**, 21–25 (2012)

Soheilmoghaddam, M., Wahit, M.U., Yussuf, A.A., Al-Saleh, M.A., Whye, W.T.: Characterization of bio regenerated cellulose/sepiolite nanocomposite films prepared via ionic liquid. Polym. Test. **33**, 121–130 (2014)

Šupová, M., Martynková, G.S., Barabaszová, K.: Effect of nanofillers dispersion in polymer matrices: a review. Sci. Adv. Mater. **3**, 1–25 (2011)

Szczepanik, B., Słomkiewicz, P., Garnuszek, M., Czech, K., Banaś, D., Kubala-Kukuś, A., Stabrawa, I.: The effect of chemical modification on the physico-chemical characteristics of halloysite: FTIR, XRF, and XRD studies. J. Mol. Struct. **1084**, 16–22 (2015)

Takahashi, N., Kuroda, K.: Materials design of layered silicates through covalent modification of interlayer surfaces. J. Mater. Chem. **21**, 14336–14353 (2011)

Taxiarchou, M., Douni, I.: The effect of oxalic acid activation on the bleaching properties of a bentonite from Milos Island, Greece. Clay Miner. **49**, 541–549 (2014)

Thomas, N.R.: Frederic Stanley Kipping-Pioneer in silicon chemistry: his life & legacy. Silicon **2**, 187–193 (2011)

Tjong, S.C.: Structural and mechanical properties of polymer nanocomposites. Mater. Sci. Eng. R Rep. **53**, 73–197 (2006)

Vaia, R.A., Ishi, H., Giannelis, E.P.: Synthesis and properties of two-dimensional nanostructures by direct intercalation of polymer melts in layered silicates. Chem. Mater. **5**, 1694–1696 (1993)

Velde, B.: Clay Minerals A Physico-Chemical Explanation of their Occurrence (1985)

Verdejo, R., Barroso-Bujans, F., Rodriguez-Perez, M.A., Antonio de Saja, J., Lopez-Manchado, M.A.: Functionalized graphene sheet filled silicone foam nanocomposites. J. Mater. Chem. **18**, 2221–2226 (2008)

Wang, K., Bahlouli, N., Addiego, F., Ahzi, S., Rémond, Y., Ruch, D., Muller, R.: Effect of talc content on the degradation of re-extruded polypropylene/talc composites. Polym. Degrad. Stab. **98**, 1275–1286 (2013)

Weissenbach, K., Mack, H.: Functional fillers for plastics. In: Silane Coupling Agents, in Functional Fillers for Plastics, pp 57–83. Wiley-VCH Verlag GmbH & Co. KGaA (2005)

Witucki, G.: A silane primer—chemistry and applications of alkoxy silanes. J. Coat. Technol. **65**, 57–60 (1993)

Xie, Y., Hill, C.A.S., Xiao, Z., Militz, H., Mai, C.: Silane coupling agents used for natural fiber/polymer composites: a review. Compos. Part A Appl. Sci. Manuf. **41**, 806–819 (2010)

Xie, A., Yan, W., Zeng, X., Dai, G., Tan, S., Cai, X., Wu, T.: Microstructure and antibacterial activity of phosphonium montmorillonites. Bull. Korean Chem. Soc. **32**, 1936–1938 (2011)

Yeh, M.-H., Hwang, W.-S.: High mechanical properties of polychloroprene/montmorillonite nanocomposites. Mater. Trans. **47**, 2753–2758 (2006)

Yui, T., Fujii, S., Matsubara, K., Sasai, R., Tachibana, H., Yoshida, H., Takagi, K., Inoue, H.: Intercalation of a surfactant with a long polyfluoroalkyl chain into a clay mineral: Unique orientation of polyfluoroalkyl groups in clay layers. Langmuir **29**, 10705–10712 (2013)

Yürüdü, C., S I., Ünlü, C., Atici, O., Ece ,Ö.I., Güngör, N.: Synthesis and characterization of HDA/ NaMMT organoclay. Bull. Mater. Sci. **28**, 623–628 (2005)

Zeng, Q.H., Yu, A.B., Lu, G.Q., Paul, D.R.: Clay-based polymer nanocomposites: research and commercial development. J. Nanosci. Nanotechnol. **5**, 1574–1592 (2005)

Zhao, Y., Zhang, S.L., Zhang, C.F., Zhou, Z., Wang, G.B.: Study on poly(ether ether ketone)/ organically modified montmorillonite composites. Plast. Rubber Compos. **38**, 279–283 (2009)